ELSEVIER

Journal of Controlled Release 82 (2002) 289–307

journal of controlled release

www.elsevier.com/locate/jconrel

Characterization of the initial burst release of a model peptide from poly(D,L-lactide-co-glycolide) microspheres

Juan Wang[a,1], Barbara M. Wang[a,2], Steven P. Schwendeman[b,*]

[a]*Pharmaceutical Analytical and Development Department, Novartis Pharmaceuticals Corp., 59 Route 10, East Hanover, NJ 07936, USA*

[b]*Department of Pharmaceutical Sciences, The University of Michigan, 428 Church Street, Ann Arbor, MI 48109-1065, USA*

Received 29 March 2002; accepted 21 May 2002

Abstract

In order to study the mechanism of initial burst release from drug-loaded poly(D,L-lactide-co-glycolide) (PLGA) microspheres, a model peptide, octreotide acetate, was encapsulated in PLGA 50/50 (M_w~50,000) microspheres using a double emulsion–solvent evaporation method. A simple and accurate continuous monitoring system was developed to obtain a detailed release profile. After different incubation times in the release medium, the morphology and permeability of the microspheres were examined using scanning electron and confocal microscopy (after immersing the microspheres in a fluorescent dye solution for 30 min), respectively. Both the external and internal morphology of the microspheres changed substantially during release of >50% of the peptide over the first 24 h into an acetate buffer, pH 4 at 37 °C. After 5 h, a 1–3 μm ''skin'' layer with decreased porosity was observed forming around the microsphere surface. The density of the ''skin'' appeared to increase after 24 h with negligible surface pores present, suggesting the formation of a diffusion barrier. Similar morphological changes also occurred at pH 7.4, but more slowly. Correlated with these results, the confocal microscopy studies (at pH 4) showed that the amount of dye penetrated inside the microspheres sharply decreased with time. In summary, over the first 24 h of drug release, a non-porous film forms spontaneously at the surface of octreotide acetate-loaded PLGA microspheres in place of an initially porous surface. These rapid alterations in polymer morphology are correlated with a sharp decline in permeability and the cessation of the initial burst.

Keywords: Biodegradable microspheres; Initial burst; Continuous monitoring; Release profile; Permeability

1. Introduction

Injectable biodegradable microspheres [e.g., poly-(D,L-lactide-co-glycolide) (PLGA) microspheres] control the release of drugs over a period of several weeks to several months. These products are generally administered through intramuscular (i.m.) or subcutaneous (s.c.) injections. Drugs that require prolonged treatment but have a short biological half-life

*Corresponding author. Tel.: +1-734-615-6574; fax: +1-734-615-6162.

E-mail address: schwende@umich.edu (S.P. Schwendeman).

[1]Current address: Alkermes, Inc., 64 Sidney Street, Cambridge, MA 02139, USA.

[2]Current address: HGB International Ltd., P.O. Box 588, Berkeley Heights, NJ 07922, USA.

0168-3659/02/$ – see front matter
PII: S0168-3659(02)00137-2

or poor oral bioavailability (e.g., peptides and proteins) are suitable candidates for microsphere delivery. Since this technology provides unique advantages over traditional delivery approaches (e.g., improved drug efficacy and patient compliance), many products are currently under development. However, there are only three products that have received regulatory approval in the United States (i.e., Lupron Depot from Takeda/TAP, Sandostatin LAR™ Depot from Novartis, and Human Nutropin™ Depot from Alkermes/Genentech).

Currently, injectable microspheres still suffer from two major technical problems. First, the rapid release during the first day or so of release typically accounts for 10~80% of the total drug loading. This so-called ''initial burst'' phenomenon poses a serious toxicity threat and is a major hurdle for the development of microsphere products. Secondly, microspheres tend to have a very slow (close to zero) release period after the initial burst period. This period usually lasts for days to weeks and is often referred to as the ''lag-time'' (or induction) period. During this lag time, the patient may not be effectively treated due to the lack of sufficient drug release.

Few studies have focused on the mechanism of the initial burst and lag time. The initial burst is widely believed to be the result of rapid release of drug from the microsphere surface [1–4], whereas the depletion of drug at the surface causes the cessation of initial burst. The lag period then starts and lasts until extensive degradation of the polymer occurs [2].

Evaluation of initial burst requires in-vitro release monitoring similar to dissolution testing. Traditional dissolution testing for conventional controlled-release dosage forms requires multiple data points (i.e., 7–10 samplings) in order to assure the drug is released in a controlled fashion over the entire release period. For controlled-release microspheres, most literature reports have inherited this traditional dissolution–sampling scheme. However, due to much longer release duration of biodegradable microspheres (e.g., 1 month), the sampling frequency within the same time frame typically used is much lower. For example, only very few samples (e.g., 1–3) are normally taken during the first day, and even fewer during the following period. Previously, an in vitro dissolution method using a microdialysis sampling technique was developed for injectable microspheres which employed a short sampling interval (~every 20 min) [5]. However, this system is difficult to set up and calibrate, which may hinder its widespread use.

Initial release kinetics and microsphere morphology information may be essential to elucidate the mechanism of initial burst and lag time. To obtain an accurate release rate profile, continuous monitoring of drug release is necessary. Unfortunately, there are few literature reports of the use of a convenient system to monitor microsphere release continuously. In addition, the information in the literature concerning microsphere morphology and permeability during the initial release period is also limited.

Therefore, the objectives of this study were to: (1) develop a continuous monitoring system to obtain a real-time microsphere release profile during the initial burst period, (2) evaluate the structural and permeability changes of microspheres during the initial drug release period, and (3) correlate the structural and permeability changes with the continuous drug release rate profile.

2. Materials and methods

2.1. Materials

Octreotide acetate (batch No. 92072), a cyclic octapeptide, somatostatin analog, was provided by Novartis Pharmaceutical Corp. PLGA 50/50 (molecular weight, M_w 53,600) was purchased from Birmingham Polymers (Birmingham, AL, USA, lot number D98083). Methylene chloride, acetonitrile, and tetrahydrofuran (THF) were purchased from Aldrich (Milwaukee, WI, USA). Polyvinyl alcohol (PVA, 88 mol% hydrolyzed, M_w 25,000) was obtained from Polysciences (Warrington, PA, USA). Filter paper (nylon, 0.45 μm) was purchased from Micron Separations (Westboro, MA, USA). Glacial acetic acid (USP grade), sodium hydroxide (NaOH) and sodium azide were obtained from Fisher Scientific (Fair Lawn, NJ, USA), sodium bicarbonate ($NaHCO_3$) from Mallinckrodt (Paris, KY, USA), and ethylenediaminetetraacetic acid disodium salt (EDTA) from Sigma (St. Louis, MO, USA). Carboxytetramethylrhodamine (CTMR, M_w 467) and dex-

tran tetramethylrhodamine (dextran TMR, M_w 3000) were purchased from Molecular Probes (Eugene, OR, USA). Unless otherwise stated, all chemicals were used as received.

2.2. Preparation of microspheres

Microspheres were prepared using a double emulsion–solvent evaporation method. Octreotide acetate (50 mg) was dissolved in 100 μl of water. The solution was mixed with 2 ml of PLGA methylene chloride solution (300 mg/ml) and emulsified by homogenization using a Vitris ''23'' homogenizer (The Vitris Company, Gardiner, NY, USA) at maximum speed for 1 min. The emulsion stabilizer (2 ml of 1% PVA solution) was then added and the mixture was vortex mixed with a Vortex Genie 2™ (Scientific Industries, Bohemia, NY, USA) at the maximum speed for 30 s. The emulsion formed was immediately poured into 100 ml of 0.3% PVA aqueous solution, which was stirred at 600 rpm. After evaporation of methylene chloride for 3 h, the microspheres were collected by filtration through 0.45 μm nylon filter paper, washed with 100 ml water three times and vacuum dried for 48 h. Microspheres were stored at 4 °C before further investigation. Blank microspheres were prepared with no octreotide acetate added to the inner water phase.

2.3. Set-up of continuous monitoring system

The schematic diagram of the system is shown in Fig. 1. The mobile phase was circulated through a high-performance liquid chromatography (HPLC) pump (600E pump, Waters, Milford, MA, USA), a HPLC UV detector (490E programmable multi-wavelength detector, Waters) and the drug release reservoir in sequence. A plastic tubing (0.02 in. I.D., UpChurch Scientific, Oak Harbor, WA, USA) with a solvent inlet filter (Waters, part No. 613609) was used to withdraw the mobile phase from the drug release reservoir (1 in.=2.54 cm). The mobile phase was then transferred from the pump to the HPLC detector with stainless steel 0.009 in. tubing, and then from the detector back to the drug release reservoir with the 0.02 in. tubing. A computer

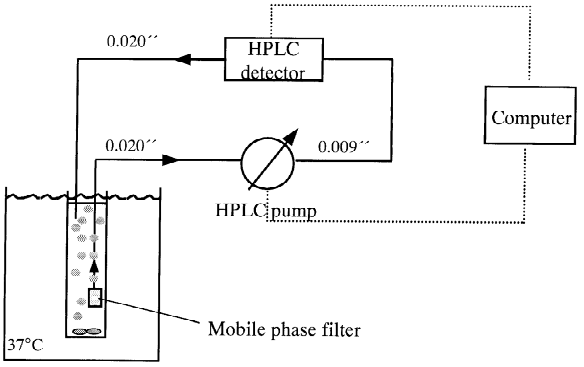

Fig. 1. Schematic diagram of instrumental set-up for continuous monitoring of the initial burst from biodegradable microspheres by using a modified HPLC system. The set-up consists of a drug release reservoir, a HPLC detector, a HPLC pump, and a computer with data acquisition system.

connected to the UV detector and the pump was used as the central control device. Millennium 32 software (Waters) was installed to control the pump flow rate and acquire the data from the UV detector. The flow rate was 1 ml/min. The data acquisition rate was 1 point/s.

A glass tube (17 mm I.D.) was used as the drug release reservoir with 20 ml of release medium (0.05 M sodium acetate buffer, pH 4) [6]. A pH of 4 was selected for the release buffer since the peptide is unstable at neutral pH. The glass tube was maintained at 37 °C in a water bath. In one instance, a pH 7.4 buffer was used (0.05 M sodium phosphate) to determine if the morphological changes observed at pH 4 were also applicable at pH 7.4. The release medium was magnetically stirred at 200 rpm. The continuous monitoring system was flushed with clean release medium before the experiment. After the system was clean (i.e., baseline was stable), the drug release reservoir was connected and the system was allowed to equilibrate with the release medium which was maintained at 37 °C. At this time, the outflow from the detector was directed into the drug release reservoir to circulate through the entire system. After equilibrium was reached again, 50 mg of drug-loaded microspheres were added into the drug release reservoir. Data collection commenced immediately and continued for 24 h. UV absorbance was monitored at both 254 and 280 nm.

2.4. Data analysis

Raw data files in Millennium 32 were exported as ASCII files and later converted into Microsoft Excel files. In order to minimize data fluctuation resulting from instrument noise, the absorption values were averaged for every minute before further processing.

2.5. Measurement of dead volume

The volume between drug release reservoir and the HPLC detector cell needs to be taken into account as part of the overall volume of the release medium. This volume was defined as dead volume. It was determined by multiplying the flow rate and the time to transfer a drug containing solution from drug release reservoir to the detector cell. The transfer time was determined by first equilibrating the detector cell with a drug-containing solution. Equilibration was assured when the UV absorbance variation was less than 1% in a 1-min interval at 280 nm. Then the first drug-containing solution was displaced and a second drug-containing solution at a different drug concentration was replaced. The time (t_1) for the switching was immediately recorded. Monitoring was continued until equilibration was reached again. From the recorded UV absorbance data on the computer, the time when the inflection point occurred on the plot (t_2) was determined. The time difference (t_2-t_1) was used as the time for transferring a solution from reservoir outlet to the detector cell. Drug-containing solutions were prepared at five different octreotide acetate concentrations (~0–0.25 mg/ml) using release medium. The dead volume was determined to be 2.92±0.08 ml ($n=5$, mean±S.D.) independent of the drug concentration used.

2.6. Determination of drug concentration in the release medium

When there is interference (I) present in the release medium, the drug concentration can be determined by monitoring the absorbance at two different wavelengths and subtracting the background absorbance. To quantify octreotide acetate (O), UV absorbance was monitored at both 254 and 280 nm. According to Beer's Law, the overall absorbance (A_{254} and A_{280}) in the release medium at these two wavelengths is:

$$A_{254} = \epsilon_{254O} \cdot C_O \cdot l + \epsilon_{254I} \cdot C_I \cdot l \quad (1)$$

$$A_{280} = \epsilon_{280O} \cdot C_O \cdot l + C_I \cdot l \quad (2)$$

where ϵ, C, and l are the absorption coefficient at either 254 or 280 nm for octreotide acetate (O) or interference (I), concentration of octreotide acetate (O) or interference (I) in release medium, and the width of the detector cell, respectively. From Eq. (1), we obtain:

$$C_I = \frac{A_{254} - \varepsilon_{254O} \cdot C_O \cdot l}{\varepsilon_{254I} \cdot l} \quad (3)$$

Substituting Eq. (3) into Eq. (2), we obtain:

$$C_O = \frac{A_{280} - \dfrac{\varepsilon_{280I}}{\varepsilon_{254I}} \cdot A_{254}}{l \cdot \left(\varepsilon_{280O} - \dfrac{\varepsilon_{280I}}{\varepsilon_{254I}} \cdot \varepsilon_{254O} \right)} \quad (4)$$

If we define $\epsilon_{280I}/\epsilon_{254I}$ as a constant R_1, Eq. (4) can be re-written as:

$$C_O = \frac{A_{280} - R_1 \cdot A_{254}}{(A_{280O\_sd} - R_1 \cdot A_{254O\_sd})/C_{O\_sd}} \quad (5)$$

where A_{280O_sd}, A_{254O_sd} are the absorbances of octreotide acetate standard solution at 280 and 254 nm and C_{O_sd} is concentration of octreotide acetate in the standard solution. If we define $(A_{280O\_sd} - R_1 \cdot A_{254O\_sd})/C_{O\_sd})$ as a constant R_2, we finally have:

$$C_O = \frac{A_{280} - R_1 \cdot A_{254}}{R_2} \quad (6)$$

Two conditions need to be satisfied in order to use dual wavelength measurement to correct for interference: (1) the ratio of the extinction constants of interference at these two wavelengths (R_1) is constant over the entire drug release period; and (2) the ratio of the extinction constants of active compound at these two wavelengths should be significantly different from R_1. Both conditions were met for octreotide acetate-loaded PLGA microspheres (data not shown).

R_1 was determined to be 0.697 ($n=86{,}400$, S.D.$=$ 0.007) by monitoring UV absorbance of blank microspheres at 280 and 254 nm for 24 h. R_2 was

determined to be 2.27 ml/mg ($n=4$, S.D.$=0.25$) using octreotide acetate standard solution at different concentrations (0–0.25 mg/ml) and $R_1=0.697$. The absorbance at each wavelength was averaged at every minute interval before further calculation.

2.7. Determination of drug loading inside plga microspheres and particle size distribution

A 15-mg amount of microspheres was dissolved in 2 ml of THF and the mixture was shaken and sonicated. After a clear solution was obtained, 8 ml of dilution solution (containing 0.2%, w/v, glacial acetic acid, 0.2%, w/v, sodium acetate, and 0.7%, w/v, sodium chloride) was added. The mixture was allowed to settle for 20 min while the polymer precipitated. The solution was filtered through a 0.45 μm PTFE filter and the sample was injected directly into the HPLC system and detected at 280 nm [6]. The theoretical loading of the microspheres was 7.7% (w/w).

The particle size distribution was analyzed by a MasterSizer X (Malvern Instruments, Southborough, MA, USA). The microspheres were suspended in 0.1% aqueous Tween 80 solutions, sonicated for 30 s and stirred for 2 min before analysis. Results are reported as volumetric mean diameters (mean±S.D., $n>1000$).

2.8. Calculation of the cumulative fraction released

The fraction of drug released at each time point, F, can be calculated as:

$$F=\frac{C_O\cdot(V_1+V_D)}{WL} \quad (7)$$

where V_1, V_D, W, and L are the volume of liquid in the release reservoir, dead volume, weight of the microspheres, and loading of drug in the microspheres, respectively.

2.9. Calculation of release-rate profile

The release rate profile was calculated by averaging the rate of change of cumulative fraction released over every 5-min interval and then plotted versus the mid-point of the interval.

2.10. Simulation of intermittent sampling results

The release rate profiles simulated at different sampling intervals were calculated by averaging the rate of change of cumulative fraction released for every 20, 60, and 240 min.

2.11. Surface and internal morphology

The external and internal morphology of microspheres was analyzed by scanning electron microscopy (SEM). Microspheres were incubated in release medium (0.05 M acetate buffer, pH 4) at 37 °C under stirring. After 0, 0.33, 1, 5, and 24 h of incubation, microspheres were recovered from the release media and freeze–dried for 4 days to remove water. The samples were mounted onto aluminium specimen stubs using double-sided adhesive tape and fractured with a razor blade. The samples were sputter coated with gold/palladium for secondary electron emissive SEM (Jeol, Tokyo, Japan).

2.12. Microsphere permeability

Microspheres were incubated in release medium at 37 °C under stirring. Individual fluorescent probe solutions were also prepared by dissolving probe CTMR (0.02%, w/w) or dextran TMR (0.2%, w/w) in release medium. After 0, 5, and 24 h, microspheres were transferred to a fluorescent probe solution at 37 °C under mild agitation at 500 rpm (Eppendorf thermomixer 5436, Brinkmann Instrument, Westbury, NY, USA). After 30 min, the mixture was settled and the supernatant was removed. The microspheres were freeze–dried overnight and examined under a confocal microscope at 543-nm excitation wavelength. Microspheres were put on a glass slide and covered with a coverslip. Images were obtained using a Bio-Rad MR/AG-1 single detector confocal laser scanning system equipped with an argon and helium neon laser (Bio-Rad Laboratories, Hercules, CA, USA). The probes were red whereas the background was black. The red signal was converted to white signal using Adobe PhotoShop 4.0 (Microsoft, Redmond, WA, USA) for better contrast. The relative permeability of microspheres as a function of time during release was evaluated by comparing the relative amount of

fluorescent dye that had penetrated into microspheres, which is correlated with the fluorescent emission from the microspheres. In order to minimize the effect of photo bleaching on the relative comparison, laser intensity was minimized and kept constant for each set of microspheres (i.e., microspheres being incubated with the same dye solution).

3. Results

3.1. Cumulative drug release and drug release rate profile from biodegradable microspheres by continuous monitoring

Microspheres formed from the solvent evaporation method were spherical, 100±57 μm in diameter (volume-average±S.D.), and had a loading efficiency of 45%. In Fig. 2A, the cumulative drug release from octreotide acetate loaded biodegradable microspheres is displayed. Experiments were repeated three times and all the profiles obtained were virtually superimposable. From the curve, it can be seen that the initial burst was high (>50%) and followed three stages: (I) a rapid release stage (the first 0.5 h), (II) a first slow release stage (from 0.5~5.5 h), and (III) a second slow release stage (from 5.5~24 h).

To clearly observe these transitions, the cumulative drug release was also plotted against the square root of time [7], as shown in Fig. 2B. It can be seen that the transitions between these stages are more distinguishable than in Fig. 2A. Both the stage II and earlier part of stage III appeared to be nearly linear, suggesting diffusion-controlled mechanisms [7]. Also, the fraction of drug release in each stage during the first day was readily ascertained. Roughly 7, 11, and 34% of drug were released during the first, second, and third stages, respectively.

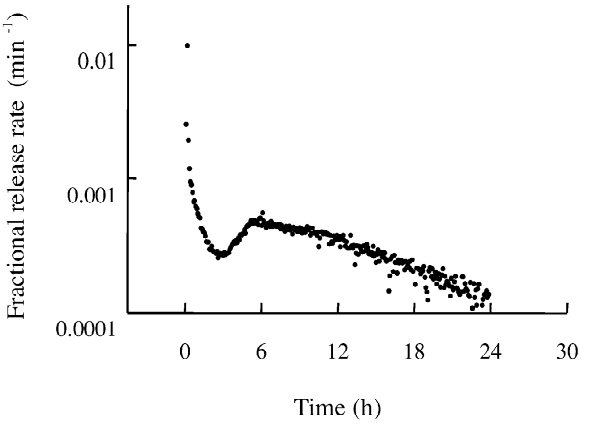

Fig. 3. Drug release rate profile from octreotide acetate loaded PLGA biodegradable microspheres.

The release rate profile of the octreotide acetate-loaded microspheres is shown in Fig. 3. Again, three stages are visible in the release curve, although the time between phase I and II, is more clearly discernible, i.e., ~3 h instead of ~0.5 h as described above. Initially, the release rate was high and dropped rapidly over the first 30 min and then less rapidly

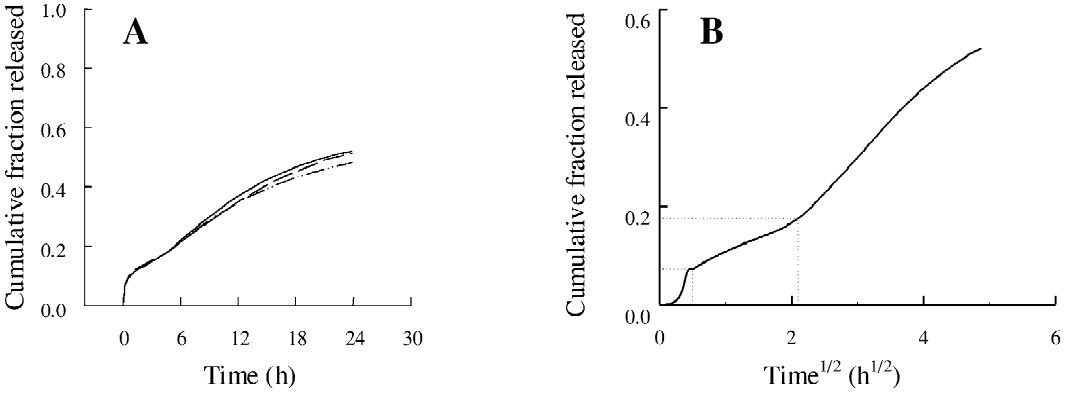

Fig. 2. Cumulative drug release from octreotide acetate loaded PLGA biodegradable microspheres in an acetate buffer (pH 4) plotted vs. time (A) and square root of time (B). The curves (— — —), (—··—), and (———) represent three independent measurements. (B) Depicts only one of the three replicates.

until reaching a minimum at around 3 h (phase I). Then, a gradual increase in release rate occurred, which reached a maximum at ~5.5 h (phase II) before the rate decreased slowly and approached zero by 24 h (phase III).

3.2. Comparing the release rate profile obtained with different sampling schedules

In most cases, intermittent sampling is used for in-vitro dissolution testing for both immediate and long-term controlled release drug delivery systems. In order to illustrate the advantages of continuous monitoring over intermittent sampling, the same data from Fig. 2A was used to simulate the results while assuming intermittent sampling had been performed at 20-min, 1-h and 4-h intervals. At each scheduled sampling point, the monitored UV absorption data was taken and used to calculate drug release.

Results are shown in Fig. 4. Cumulative drug release was still plotted versus square root time because of obvious transitions between each stage. It can be seen that when samples were taken at every 20 min, the release profile was superimposed on the curve obtained from continuous monitoring and only one curve could be observed in the graph. However, when the sampling interval increased to 1 h, the first phase and the second phase became indistinguishable. The entire release curve appeared to be sigmoidal shaped (two release phases with a gradual transition in between). When the sampling interval further increased to 4 h, the second transition became too ambiguous to interpret.

If discrete sampling were used to determine cumulative drug release over a 24-h period, the release rate profile could also be obtained by determining the derivative of the cumulative release curve interpolated between the sampling data points. In Fig. 5, the release rate profiles were plotted for the release data obtained with different sampling intervals. It was assumed that drug was released at a constant rate during each sampling interval.

As illustrated in Fig. 5, at 20-min sampling intervals, the initial drug release rate was about two-thirds lower than that determined by continuous monitoring (note that the ordinate in Fig. 5 is in log scale). The time and magnitude of the peak and valley rates, however, were not affected. When the

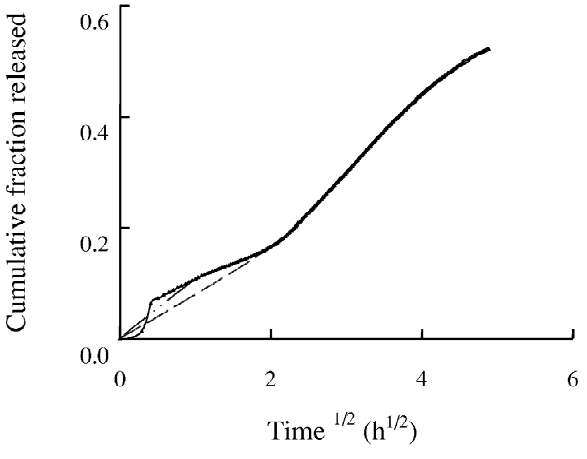

Fig. 4. Simulated cumulative drug release profiles from octreotide acetate loaded PLGA biodegradable microspheres by assuming sampling was performed at 20-min (———), 1-h (—··—), and 4-h (— — —) intervals. The results plotted from continuous monitoring (▲) were superimposed by simulated sampling curves at a 20-min interval.

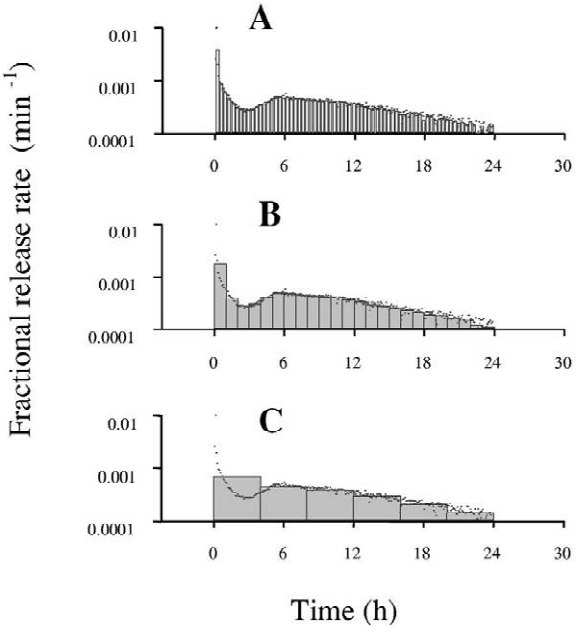

Fig. 5. Simulated drug release rate profile from octreotide acetate loaded PLGA biodegradable microspheres by assuming sampling was performed at 20-min (A), 1-h (B), and 4-h (C) intervals. The original results from continuous monitoring (·····) were also displayed for comparison.

sampling interval increased to 1 h, the first release rate was only one-fifth of that by continuous monitoring, and the release rate only showed a gradual decrease over the first 3 h. The times for the peak and valley rates were slightly shifted while the magnitudes were the same. Finally, when the sampling intervals increased to 4 h, it became impossible to distinguish between different phases in the release rate profile. The drug appears to be released from microspheres with a gradually decreasing rate for the entire 24 h.

3.3. Spontaneous external morphological changes during initial 24 h of drug release

After microspheres were incubated for different time periods, their external morphology was observed using SEM. Results are summarized in Figs. 6 and 7. Pictures were taken at low magnification (500×, Fig. 6) and high magnification (10,000×, Fig. 7). At low magnification, numerous small pores were observed on the surface of microspheres at zero time. These pores increased in number and were still

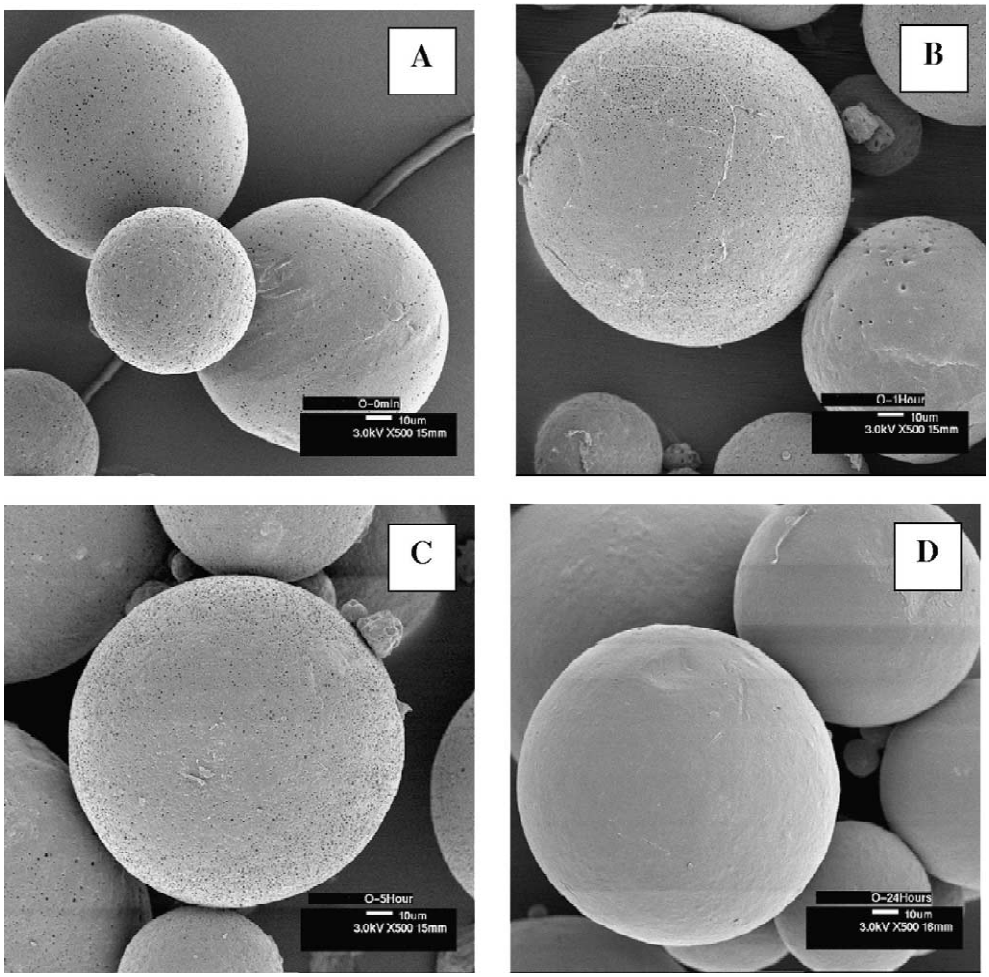

Fig. 6. Overview of external morphology of octreotide acetate-loaded PLGA biodegradable microspheres after 0-h (A), 1-h (B), 5-h (C) and 24-h (D) incubation times in the release medium at 500× magnification by SEM.

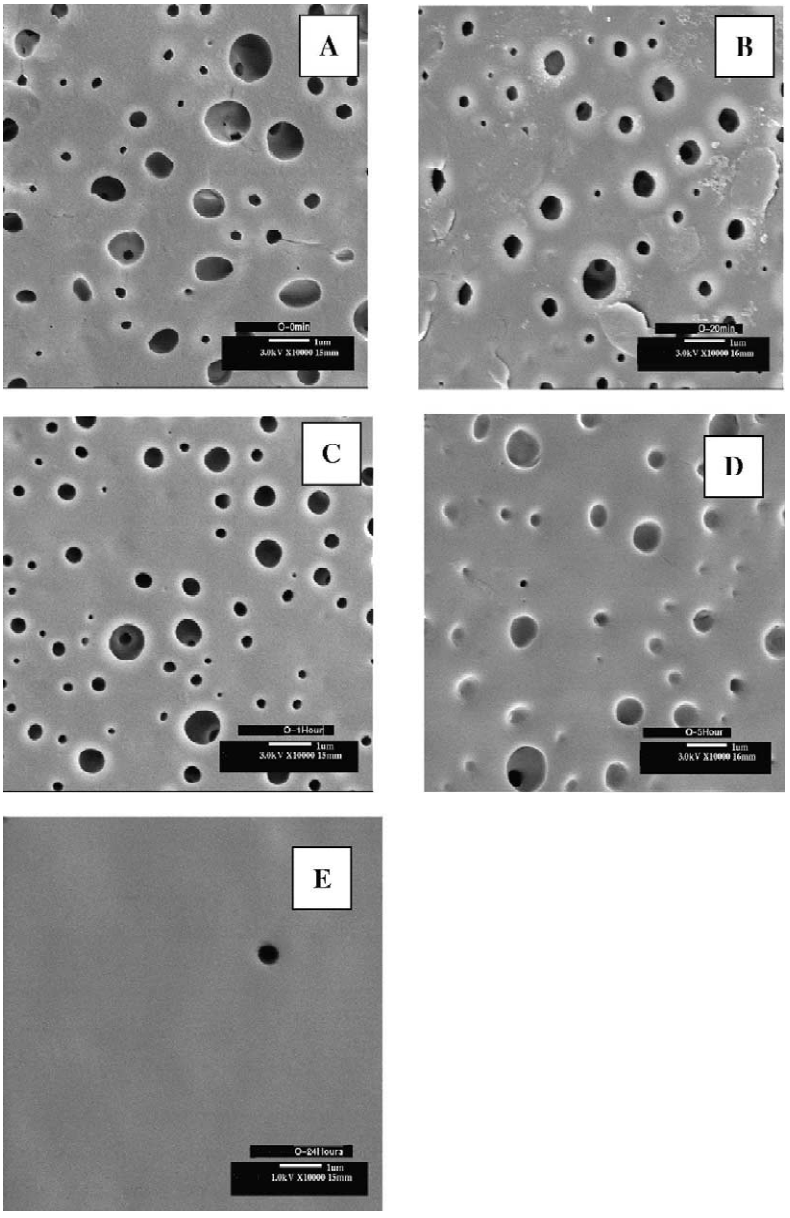

Fig. 7. External morphology of octreotide acetate-loaded PLGA biodegradable microspheres after 0-h (A), 0.3-h (B), 1-h (C), 5-h (D) and 24-h (E) incubation times in the release medium at 10,000× magnification by SEM.

present after 1 and 5 h of incubation. However, after 24 h, the microsphere surface appeared smooth as the pores on the surface had disappeared.

Using high magnification, greater detail of the microsphere surface was observed. Initially, the size of the pores ranged from 10 to 1000 nm (Fig. 7A). The connecting channels between pores on the surface and those inside microspheres can also be

observed. The surface pores ranged from irregular to round shape. After 20 min, no significant change was observed. After 1 h, only mostly round pores (no irregular shaped pores) were observed. By 5 h, the size of pores become smaller and less in number, indicating pores were closing with time. For those pores that remained open, underlying polymer structures were observed, which suggested that the pores were closing from inside out before disappearing by 1 day of incubation.

During microscopic examination, the surface of a small portion of microspheres showed a distinct boundary separating it into two distinct regions (Fig. 8). These irregular microspheres were not observed in the sample before incubation. The surface porosity of the upper portion of these microspheres resembles that observed before incubation (Fig. 6A) while the surface porosity of the lower portion of these microspheres resembles that observed after various incubation times (Fig. 6B–E). In particular, after 24 h all the pores on the ''lower'' portion disappeared, whereas those of the ''upper'' portion still resembled the original porous surface. These results indicated that these microspheres had been suspended at the

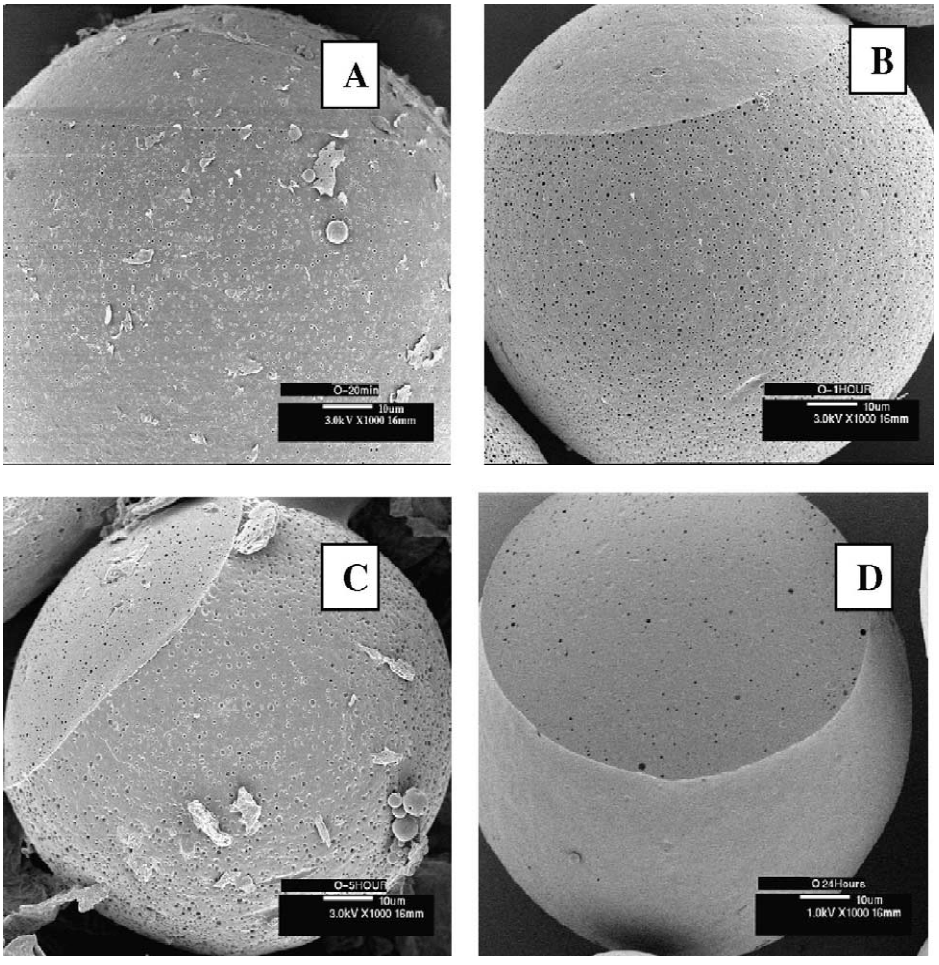

Fig. 8. External morphology of ''floating'' octreotide acetate-loaded PLGA biodegradable microspheres after 0.3-h (A), 1-h (B), 5-h (C) and 24-h (D) incubation times in the release medium at 1000× magnification by SEM.

liquid/air interface during incubation (i.e., ''floating'' microspheres). The boundary separated the above water (''upper'') and below water (''lower'') portions of the microsphere. The apparent diameter of the ''lower'' portion was larger as compared to the ''upper'' portion, and increased with time, indicative of polymer swelling kinetics.

3.4. Spontaneous internal morphological changes during the first 24 h of drug release

The internal morphology of microspheres after different incubation times was examined at 4000× magnification. At zero time, numerous pores were observed inside the microspheres (Fig. 9A). The porosity was homogeneous throughout the cross-section of the microspheres. No significant change was observed after 20 min and 1 h of incubation (Fig. 9B and C). However, after 5 h, the porosity near the microsphere surface decreased significantly. A ''skin'' type structure roughly 1–3 μm thick was observed (Fig. 9D). After 24 h, the porosity of the ''skin'' decreased further whereas that of the microsphere core increased (Fig. 9E). An expanded view of the formed ''skin'' structure is shown in Fig. 9F. This picture clearly indicates that the entire microsphere is wrapped within the ''skin'' and the internal porosity is significantly higher than the peripheral porosity.

3.5. Drop-off in the permeability of microspheres

After incubation with fluorescent probes, the fluorescent intensity inside microspheres (the brightness of microspheres) was monitored as an indicator of the relative permeability of the microspheres. The confocal pictures of microspheres after incubating with aqueous solutions of a small M_w probe (CTMR, M_w 467) and a large M_w probe (TMR, M_w 3000) are shown in Figs. 10 and 11. Clearly, the intensity of probes inside microspheres decreased as incubation time increased from 0, 5, to 24 h, indicating that the permeability of microspheres followed the same order. After 24 h of incubation, almost no fluorescent probe was observed inside the microspheres, indicating permeability of microspheres was approaching a negligible value.

4. Discussion

4.1. Advantages of continuous monitoring over intermittent sampling

One of the major hurdles with the microsphere technology is its large initial burst [8–12]. In order to build a more accurate physical–chemical picture of the burst phenomena, the first-day release kinetics is required. However, release testing for microsphere products have been largely dominated by traditional sampling techniques (i.e., 3–4 sampling times during the first day and 1 sampling/day or less for the subsequent days) followed by off-line analysis (e.g., UV–Vis spectrophotometry or HPLC). This traditional technique does not provide detailed and accurate drug release kinetics, as demonstrated in Figs. 4 and 5. On the other hand, as shown in Figs. 2A and 3, both the cumulative release profile and the release rate profile obtained from continuous monitoring showed several distinct stages, which suggested different release mechanisms dominating drug release within the first 24 h. Similar kinetic behavior was reported previously using a microdialysis technique at a 20-min sampling interval [5].

4.2. Advantages of continuous monitoring based on HPLC detector over traditional continuous flow monitoring based on UV–Vis spectrophotometry

Since the 1960s, various continuous-flow dissolution-testing systems have been proposed [13]. Most of such systems used peristaltic or proportioning pumps to circulate fluids in a closed or open system [14]. In some of these devices, release medium was circulated continuously through a UV spectrophotometer flow cell for on-line monitoring [15,16]. However, in others, the release medium was transferred frequently into a flow cell and the UV absorbance was measured at a static condition [16]. The latter approach is also called the continuous flow sampling method [13] and is preferred over on-line monitoring because it allows the contents of the cell to stabilize (e.g., flow to stop) before reading the absorbance [17]. Since the emergence and popularity of HPLC technology, many recent publications use off-line HPLC testing combined with manual or automatic sampling for drug release testing.

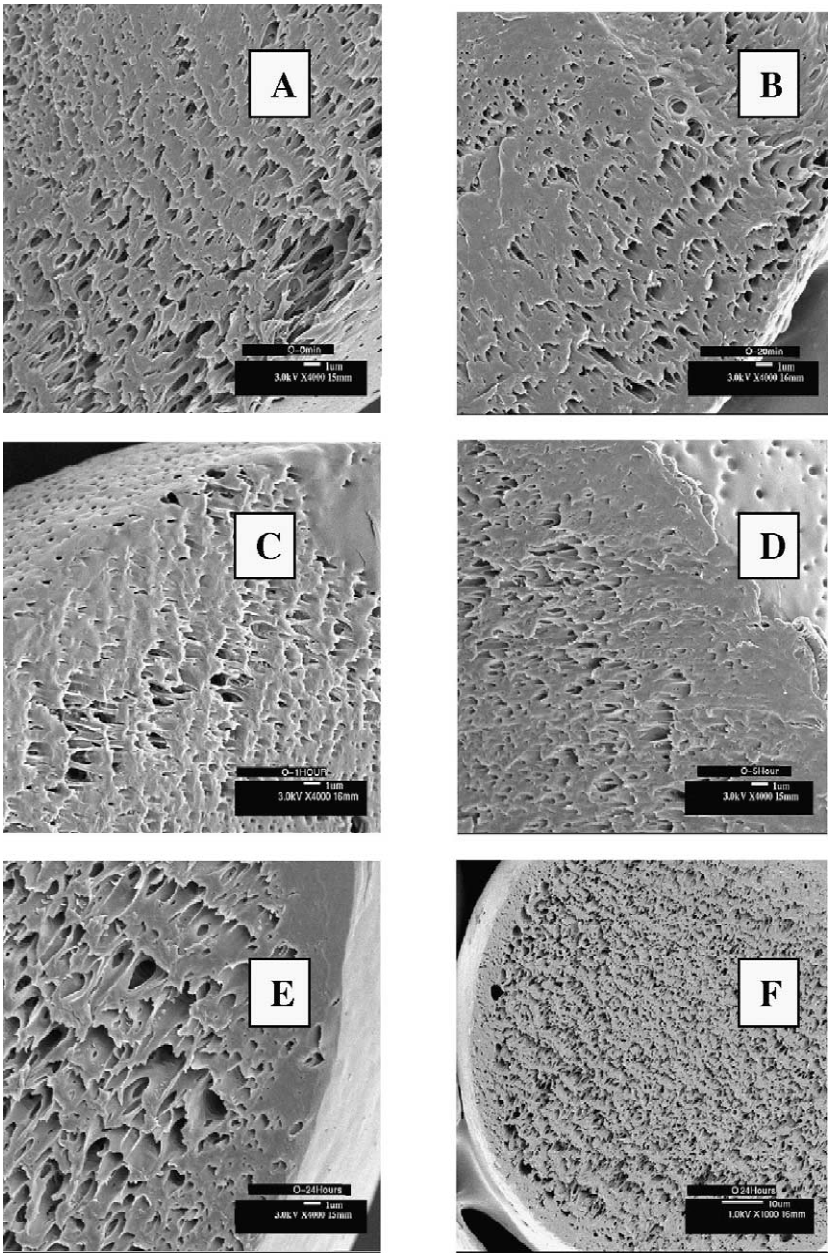

Fig. 9. Internal morphology of octreotide acetate-loaded PLGA biodegradable microspheres after 0-h (A), 0.3-h (B), 1-h (C), 5-h (D) and 24-h (E and F) incubation times in the release medium at 4000× (A through E) and 1000× (F) magnification by SEM.

However, these traditional continuous monitoring devices invariably use UV spectrometers for detection. The flow cell in most UV spectrometers has a volume of around 0.2 to 1 ml. For continuous monitoring, the large volume of the flow cell poses a significant problem. Firstly, the fluid entering the flow cell is mixed with the previous volume that reduces sensitivity and requires a large flow rate to compensate for this problem. Secondly, the rectangular shape of the flow cell can cause disturbances to

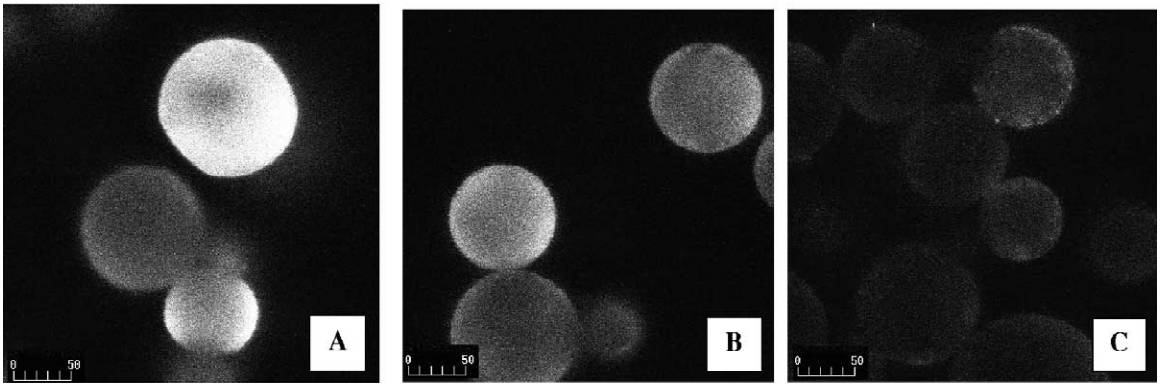

Fig. 10. Cross-sectional view of octreotide acetate-loaded PLGA biodegradable microspheres after 0-h (A), 5-h (B), and 24-h (C) incubation times in the release medium and treated with CTMR (M_w 467) aqueous solution for 30 min using the confocal microscope at 543 nm excitation wavelength. Images were treated with Adobe PhotoShop to convert red color into white color for better contrast. Scale unit is μm.

the continuous flow. As a result, various designs of continuous flow cells employed smaller volume and optimized shape. Despite all those modifications, traditional UV spectrometer-based continuous monitoring systems require large flow (e.g., >10 ml/min). Such devices are suitable for large-scale testing (e.g., tablet dissolution test) but cannot be used for small-scale laboratory research and development studies, which require a small flow rate to accommodate a limited sample size.

The continuous monitoring system used in this study was modified from the widely available HPLC system and is simple to set up. The HPLC detectors are designed for on-line monitoring with a broad range of flow rates (e.g., 0–10 ml/min). The flow cells in the HPLC detectors were optimized for maximum sensitivity and minimum void volume. The shape of the flow cell was also designed to minimize sample diffusion within the flow cell caused by flow conditions, which may broaden the peak. The volume of the flow cell was significantly smaller than that used in UV spectrometers (e.g., 12 μl or smaller versus 200 μl). All these characteristics make HPLC detectors more suitable than UV spectrometers for on-line monitoring, especially when the quantity of the test sample is limited. For micro-

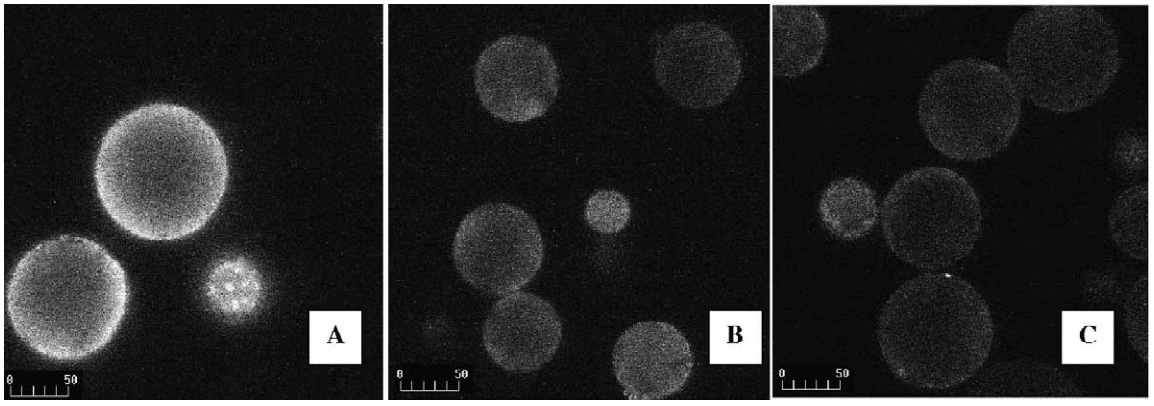

Fig. 11. Cross-sectional view of octreotide acetate-loaded PLGA biodegradable microspheres after 0-h (A), 5-h (B), and 24-h (C) incubation time periods in the release medium and treated with dextran TMR (M_w 3000) aqueous solution for 30 min using the confocal microscope at 543 nm excitation wavelength. Images were treated with Adobe PhotoShop to convert red color into white color for better contrast. Scale unit is μm.

sphere release testing for a laboratory-scale batch, the traditional UV–Vis spectrophotometer-based continuous monitoring system would not be suitable due to the much lower sensitivity.

4.3. Limitation of current continuous monitoring system modified from a HPLC system

Compared to off-line analysis where the samples could be saved and analyzed together, on-line monitoring performs sample collection and analysis throughout the experimental duration. Therefore, the instrument (in our case, the HPLC detector and pump) needs to be maintained at stable conditions during a relatively long period. Since the flow for modern HPLC pumps is fairly stable for long periods, the drifting of the HPLC detector may become the limiting factor for our custom designed system. (The influence of noise level of the UV detector can be smoothed out by averaging multiple readings and is not so critical). This is especially the case when the release rate is small. Generally, one can consider the interference from detector drifting as insignificant if the following condition is satisfied:

$$D_f \times 10 \leq \frac{\varepsilon l(ML/V)(R_2 - R_1)}{t_2 - t_1} \quad (8)$$

where D_f, ϵ, l, M, L, V, R_2, and R_1 are the detector drifting (may be determined experimentally or estimated using specification value from supplier), extinction coefficient of the drug molecule, the length of detector cell (usually 1 cm), sample amount, drug loading in microspheres, total volume of the continuous monitoring system, percent drug release from microspheres at times t_2 and t_1, respectively. The value of 10 is an arbitrary factor, which arises from the assumption that the interference from detector drifting should be less than one tenth of drug release. Obviously, one can increase sample amount and/or decrease the total volume of the continuous monitoring system to counter the interference from detector drifting.

Another built-in parameter for our custom designed continuous monitoring system is the dead volume, which is the total volume minus the volume of drug release reservoir. This consists of volume in the HPLC pump and that of all the connecting tubing. The volume of detector cell can be ignored. Since the detector cell measures the difference in drug concentration in drug release reservoir, the dead volume would always have a delay effect on this measurement due to incomplete mixing. Therefore, while the release rate is large, the limiting factor becomes the relative ratio of dead volume versus the volume of the drug release reservoir. Usually, the influence of dead volume can be countered by increasing the flow rate of the system.

4.4. Influence of morphological changes of microspheres on drug release during initial 24 h

In order to understand the relationship between initial drug release and the structure of microspheres, this study examined the morphological changes during the first 24 h of release in detail and its correlation with the drug release rate profile. Currently, the most commonly used encapsulation method to prepare microspheres is the solvent evaporation method, which often involves the formation of a double water–oil–water (w/o/w) emulsion when encapsulating peptides and proteins. Therefore, this study focused on microspheres prepared by this method using a highly water-soluble peptide. Other encapsulation methods might result in significantly different morphologies and are not discussed here.

The structure and permeability changes of microspheres during different release phases are summarized in Fig. 12. After solvent evaporation and drying, the microsphere product prepared in this study showed numerous pores on the surface. The pore size ranged from 10 to 1000 nm, which is larger than the typical encapsulated small molecule or protein. The interconnecting channels were observed throughout the microspheres (Figs. 7A and 9A). Similar initially porous surfaces with interconnecting channels have been reported for microspheres prepared by similar methods [18,19]. Fluorescent probes (M_w: 467 and 3000) could easily diffuse into the microsphere at this initial phase, indicating a high permeability. This high permeability is consistent with the high release rate of drug at the initial time point as pointed out in Fig. 12.

Significant inter-particle variability of external and internal morphology was observed both with respect to the size of microspheres and the size and number

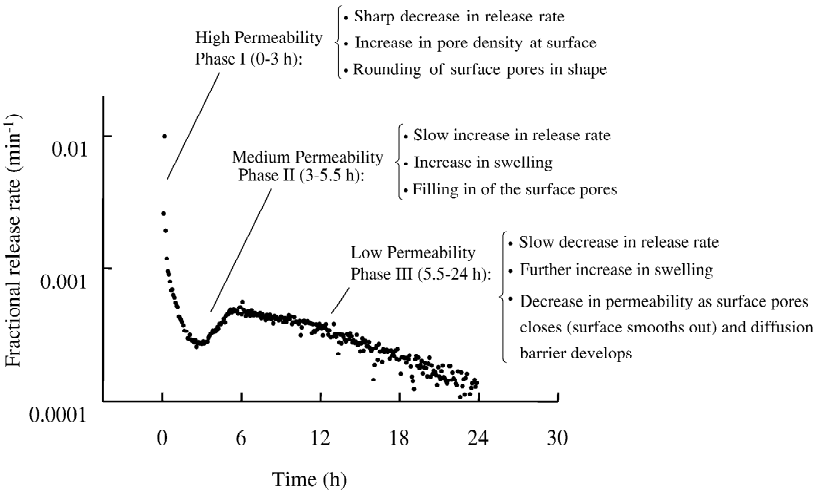

Fig. 12. Correlation of observed morphological and permeability events with the three phases of initial drug release. From octreotide acetate loaded PLGA biodegradable microspheres: phase I, a very high initial release rate followed by a sharp drop before 30 min and a slower drop between 0.5 and 3 h; phase II, slow increase of release rate between 3 and 5.5 h; and phase III, slow decrease of release rate during 5.5–24 h.

of the pores on the microsphere surface and interior. As a result, subtle morphological differences from 0 to 20 min of incubation cannot be distinguished by comparing external SEM pictures of different microspheres (e.g., Fig. 6A and B and Fig. 7A and B). In addition, the extent of swelling after different periods of incubation cannot be visually confirmed. However, the ''floating'' microspheres provided an intraparticle comparison. The ''upper'' portion gave the initial porosity, whereas the ''lower'' portion gave the porosity after various times of incubation. From these ''floating'' microspheres, we found that the diameter and number of surface pores increased shortly after the start of incubation (Fig. 8A). Drug leaching out from the surface (unplugging pores) or the rupture of surface polymer structure due to osmotic pressure could be possible causes of this phenomenon. The sharp drop in release rate after 30 min suggested the depletion of drug molecules that are immediately accessible for release. This population may include drug molecules at the periphery of microspheres and/or at the aqueous channels inside microspheres. The extent of swelling is available by comparing the relative diameter of ''upper'' and ''lower'' portions. The use of ''floating'' microspheres was found useful for studying the changes in size and shape of microspheres.

Between 20 min and 5.5 h, the rate of drug release experienced a local minimum and a local maximum, indicating that other drug release mechanism(s) were involved in addition to simple diffusion from the surface of microspheres. During this period, the external pores on the surface of microspheres began to smooth out in the perimeter (Fig. 7C) and reduce in size and number (Fig. 7D). At the same time, the internal structure of microspheres showed a porous core and a much less porous surface (''skin'' type structure) (Fig. 9D). This morphological change correlated with the reduced permeability at 5 h compared with the zero time point (Fig. 9A and B). However, even though the reduced permeability of microspheres might explain the further decrease in release rate during the later stage of phase I, the cause for increase in release rate during phase II (between 3 and 5.5 h) is not clear. Possible reasons include: (1) uptake of water in the polymer matrix increased effective diffusion coefficient of the peptide in the pore network, (2) more drug molecules were exposed to aqueous channels due to the polymer rearrangement, and (3) drug molecules diffused from very small pores inside microspheres after a relatively long time.

From these results, it was clear that multiple mechanisms contributed to the initial burst. Previous

reports have generally attributed the initial burst to rapid release of drug from the surface of microspheres. However, the definition of ''surface drug'' is ambiguous. Some studies defined ''surface drug'' as superficial drug [2], whereas other reports did not specify [4,10]. These data clearly showed that, no matter how the surface drug is defined (i.e., either as superficial drug or as drug at the effective surface of microspheres), it only contributed partially to the initial burst.

After 5 h of incubation (phase III), the rate of drug release started to slow down again until approaching zero by the end of the 24-h incubation. During this period, the surface porosity continued to decrease and almost no pores were visible at 24 h. The density of the ''skin'' formed at the surface of microspheres also appeared to increase, which correlated with extremely low permeability at 24 h. These results indicated that the decreased permeability of microspheres, which resulted from spontaneous polymer chain rearrangements, caused the initial burst to cease. To our knowledge, this is the first clear observation of a ''skin'' type of structure in microspheres.

4.5. Implications of initial morphological changes on further drug release and microclimate inside microspheres

The morphological studies using SEM revealed pore closing and ''skin'' formation phenomena in microspheres. Previously, a skin type structure was observed for large specimens (e.g., machined slab with dimensions $2\times10\times15$ mm) prepared from 75/25, 85/15 PLGA, and P(D,L)LA (M_w 50,000–130,000) after days to weeks of polymer degradation in phosphate-buffered saline (PBS) buffer [20–23]. By visual examination, the authors observed a membrane type structure close to the surface of the specimen whereas the center of the specimen was fluid like. This observation was explained by the higher local concentration of carboxylic acid end groups in the center causing auto-catalysis of polymer degradation. It was believed that the degradation products formed near the surface could dissolve more easily into the medium and diffuse away. Differential scanning calorimetry studies also indicated that even though the specimens were prepared using intrinsic amorphous polymers, highly crystalline regions (containing exclusively the L-lactide isomer in the polymer) formed at the surface of specimens after some period.

The initial morphological changes of microspheres have been largely overlooked. Even though it has been routinely suspected that similar preferential degradation could also happen in microspheres, there has been no visual proof to support such a hypothesis. Using gel permeation chromatography and differential scanning calorimetry, Park observed a transient multiple crystallization of D- or L-lactic acid oligomers during degradation of originally amorphous PLGA polymers. In addition, two distinctive glass transition temperatures were observed when these crystallization phenomena occurred [24]. Based on this information, Park proposed that fast- and slow-eroding polymer domains within microspheres were present transiently during degradation. However, the author expected that only the microsphere with a non-porous, smooth surface and monolithic, dense internal structure before degradation would undergo a heterogeneous bulk degradation. For microspheres prepared by a solvent evaporation method, similar degradation characteristics was not expected due to their porous internal structure [24].

In this study, even though microspheres we studied were very porous initially, we observed two polymer domains with different porosity within microspheres during the first day of drug release. Apparently, the porosity of the newly formed skin was significantly less than the original porosity close to the microsphere surface. This result indicated that polymer rearrangement caused the reduction in surface porosity, closing of pores at the surface, and formation of the skin layer.

Because octreotide acetate is unstable at neutral pH, the continuous release and morphological evaluation was performed at pH 4. Control experiments were performed at pH 7.4 using PBS in order to be certain that the same morphological changes reported here also occurred at physiological pH. As seen in Fig. 13, the external/internal morphology changes during octreotide acetate release at pH 7.4 were found to be similar to those observed at pH 4, except pore closing at the surface of the microspheres was slower (i.e., pore closing at pH 7.4 after 4 days was similar to that at pH 4 after 1 day) and

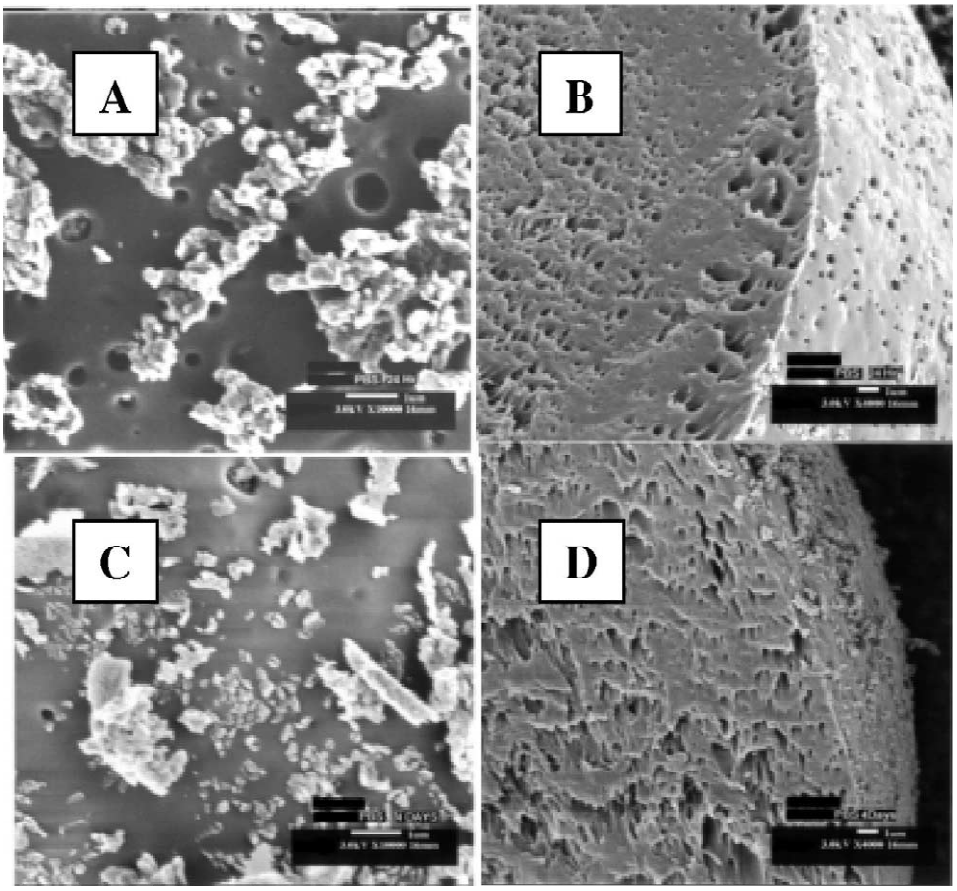

Fig. 13. External (A and B) and internal (C and D) morphology of octreotide acetate-loaded PLGA biodegradable microspheres after 1 day (A and C) and 4 days (B and D) incubation in phosphate buffer (pH 7.4) at 4000× or 10,000× magnification by SEM.

the ''skin'' layer was thinner. Thus, the surface-alteration and permeability changes occurring in octreotide acetate-loaded PLGA microspheres appear to be general phenomena irrespective of the lower pH used to stabilize the peptide in the release media. Future studies will be focused on elucidating the molecular mechanism of the spontaneous morphological changes and their relevance for in vivo drug release.

The observation of the skin structure also offers a new explanation for the lag (induction) time. In our study, near zero permeability of microspheres was observed after 24 h of drug release, which agreed with the very low rate of drug release during the lag-time period. A long-term release study for the similarly prepared microspheres showed a lag period of ~10 days after initial burst (data not shown). Evidently, if the dense skin is the cause for the lag time, then the lag time would not end until the polymer degradation progresses to a point that causes the skin to rupture. In fact, this hypothesis correlated with previous observations that the lag phase stopped when either the polymer degradation progressed to the point of erosion and break up of the polymer–drug matrix [2] or the polymer molecular weight fell below a critical value [25].

Besides affecting the rate of drug release, the formed skin structure could have significant impact on the microclimate inside microspheres, and consequently, drug stability. The microclimate pH has been shown to influence the stability of a variety of drugs inside microspheres [26–29]. The very low

permeability even for small molecular weight probes suggested that the diffusion of acidic degradation products could be greatly suppressed. In fact, acidic pH (pH 2–5) has been observed in initially porous microspheres prepared by the w/o/w process [29] and by the o/w process [27], suggesting the formation of a diffusion barrier for initially permeable microspheres.

In summary, over the first 24 h of drug release, a non-porous film was found to form spontaneously at the surface of octreotide acetate-loaded PLGA microspheres in place of an initially porous surface. This rapid alteration in polymer morphology was correlated with a sharp decline in permeability and the cessation of the initial burst. This morphological change has significant implications on the rate of drug release and maybe important for the microclimate inside microspheres.

Acknowledgements

The authors would like to acknowledge Tox-Pathology Department at Novartis and Mr. Paul Grosenstein for the help with the SEM study. This work was supported in part by a gift from Novartis Pharmaceutical Corp., and a grant from NIH (HL 68345).

References

[1] J.L. Cleland, Solvent evaporation processes for the production of controlled release biodegradable microsphere formulations for therapeutics and vaccines, Biotechnol. Prog. 14 (1998) 102–107.
[2] C.G. Pitt, The controlled parenteral delivery of polypeptides and proteins, Int. J. Pharm. 59 (1990) 173–196.
[3] R.P. Batycky, J. Hanes, R. Langer, D.A. Edwards, A theoretical model of erosion and macromolecular drug release from biodegrading microspheres, J. Pharm. Sci. 86 (1997) 1464–1477.
[4] S. Cohen, T. Yoshioka, M. Lucarelli, L.H. Hwang, R. Langer, Controlled delivery systems for proteins based on poly(lactic/glycolic acid) microspheres, Pharm. Res. 8 (1991) 713–720.
[5] A.K. Dash, P.W. Haney, M.J. Garavalia, Development of an in vitro dissolution method using microdialysis sampling technique for implantable drug delivery systems, J. Pharm. Sci. 88 (1999) 1036–1040.
[6] D. Bodmer, T. Kissel, E. Traechslin, Factors influencing the release of peptides and proteins from biodegradable parenteral depot systems, J. Controlled Release 21 (1992) 129–138.
[7] Y.W. Chien, in: Y.W. Chien (Ed.), Novel Drug Delivery Systems, Marcel Dekker, New York, 1992, pp. 1–43.
[8] H. Okada, Y. Doken, Y. Ogawa, H. Toguchi, Preparation of three-month depot injectable microspheres of leuprorelin acetate using biodegradable polymers, Pharm. Res. 11 (1994) 1143–1147.
[9] H. Okada, M. Yomanoto, T. Heya, Y. Inoue, S. Kamei, Y. Ogawa, H. Toguchi, Drug delivery using biodegradable microspheres, J. Controlled Release 28 (1994) 121–129.
[10] J.L. Cleland, A. Lim, L. Barron, E.T. Duenas, M.F. Powell, Development of a single-shot subunit vaccine for HIV-1: Part 4. Optimizing microencapsulation and pulsatile release of MN rpg 120 from biodegradable microspheres, J. Controlled Release 47 (1997) 135–150.
[11] S. Kamei, M. Yamada, Y. Ogawa, Method of producing sustained-release microcapsules, US Pat. 5,575,987, 19 November 1996.
[12] T. Yoshioka, H. Okada, Y. Ogawa, Sustained release microcapsule for water soluble drug, US Pat. 5,271,945, 21 December 1993.
[13] W.A. Hanson, in: Handbook of Dissolution Testing, Pharmaceutical Technology Publications, Springfield, OR, 1982, pp. 125–149.
[14] U.V. Banakar, in: Pharmaceutical Dissolution Testing, Marcel Dekker, New York, 1992, pp. 53–106.
[15] J.B. Johnson, P.G. Kennedy, S.H. Rubin, System for automated determination of dissolution rate, J. Pharm. Sci. 63 (1974) 1931–1935.
[16] H.M. Abdou, in: Dissolution, Bioavailability and Bioequivalence, Mack Printing Company, Easton, PA, 1989, pp. 115–144.
[17] W.A. Hanson, A.M. Paul, in: U.V. Banakar (Ed.), Pharmaceutical Dissolution Testing, Marcel Dekker, New York, 1992, pp. 107–132.
[18] Y. Ogawa, Injectable microcapsules prepared with biodegradable poly(alpha-hydroxy) acids for prolonged release of drugs, J. Biomater. Sci. (Polymer Edn.) 8 (1997) 391–409.
[19] P.P. DeLuca et al., in: M.A. El-Nokaly, D.M. Piatt, B.A. Charpentier (Eds.), Polymeric Delivery Systems, Properties and Applications, American Chemical Society, Washington, DC, 1992, pp. 53–79.
[20] S. Li, H. Garreau, M. Vert, Structure–property relationships in the case of the degradation of massive aliphatic poly-(alpha-hydroxy acids) in aqueous media, part 1: poly(DL-lactic acid), J. Mater. Sci. Mater. Med. 1 (1990) 123–130.
[21] S. Li, H. Garreau, M. Vert, Structure–property relationships in the case of the degradation of massive aliphatic poly-(alpha-hydroxy acids) in aqueous media, part 2: degradation of lactide–glycolide copolymers: PLA37.5GA25 and PLA75GA25, J. Mater. Sci. Mater. Med. 1 (1990) 131–139.
[22] S. Li, H. Garreau, M. Vert, Structure–property relationships in the case of the degradation of massive aliphatic poly-(alpha-hydroxy acids) in aqueous media, part 3: influence of the morphology of poly(L-lactic acid), J. Mater. Sci. Mater. Med. 1 (1990) 198–206.
[23] M. Vert, S. Li, H. Garreau, More about the degradation of

LA/GA-derived matrices in aqueous media, J. Controlled Release 16 (1991) 15–26.
[24] T.G. Park, Degradation of poly(lactic-co-glycolic acid) microspheres: effect of copolymer composition, Biomaterials 16 (1995) 1123–1130.
[25] F.G. Hutchinson, B.J.A. Furr, Biodegradable polymer systems for the sustained release of polypeptides, J. Controlled Release 13 (1990) 279–294.
[26] A. Shenderova, T.G. Burke, S.P. Schwendeman, Stabilization of 10-hydroxycamptothecin in poly(lactide-co-glycolide) microsphere delivery vehicles, Pharm. Res. 14 (1997) 1406–1414.
[27] A. Shenderova, T.G. Burke, S.P. Schwendeman, The acidic microclimate in poly(lactide-co-glycolide) microspheres stabilizes camptothecins, Pharm. Res. 16 (1999) 241–248.
[28] G. Zhu, S.R. Mallery, S.P. Schwendeman, Stabilization of proteins encapsulated in injectable poly(lactide-co-glycolide), Nat. Biotechnol. 18 (2000) 52–57.
[29] K. Fu, D.W. Pack, A.M. Klibanov, R. Langer, Visual evidence of acidic environment within degrading poly(lactic-co-glycolic acid) (PLGA) microspheres, Pharm. Res. 17 (2000) 100–106.